polysaccharides

MDPI

Article

Lipid-Lowering Mechanism of Lotus Root Polysaccharides in *Drosophila* Fed with a High-Fat Diet Based on Transcriptome Analysis

Chenlu Wei [1,2], Huanhuan Chen [3], Zhao Zhang [1,2], Ying Sun [1,2,*], Hongxun Wang [1,2], Xiaojuan Xu [4,*] and Yang Yi [1,2,*]

[1] College of Food Science and Engineering, Wuhan Polytechnic University, Wuhan 430023, China; weichenlu0026@163.com (C.W.); zhangz950729@163.com (Z.Z.); wanghongxun7736@163.com (H.W.)
[2] Hubei Key Laboratory for Processing and Transformation of Agricultural Products, Wuhan Polytechnic University, Wuhan 430023, China
[3] College of Food Technology, Wuhan Business University, Wuhan 430056, China; chenhuan2334@163.com
[4] College of Chemistry and Molecular Sciences, Wuhan University, Wuhan 430072, China
* Correspondence: sunying@whpu.edu.cn (Y.S.); xuxj@whu.edu.cn (X.X.); yiy86@whpu.edu.cn (Y.Y.); Tel.: +86-15171507535 (Y.S.)

Abstract

Our previous work has proved that lotus root polysaccharide has good lipid-lowering activity in vitro. In this work, we further investigated the lipid-lowering activity of lotus root polysaccharides in vivo and explored the underlying mechanism. The effects of two lotus root polysaccharides LRW (lotus root polysaccharide by water extraction) and LRA (lotus root polysaccharide by alkali extraction) on the food intake, lifespan, and lipid-lowering activity in *Drosophila melanogaster* induced by a high-fat diet were compared, and the lipid-lowering mechanism of lotus root polysaccharides was explored based on gene sequencing technology. The results showed that both LRW and LRA significantly prolonged the average lifespan of high-fat-diet-fed *Drosophila*, with more pronounced longevity-promoting effects observed for LRA. Medium- and high-dose interventions (5 and 10 mg/mL) of LRW and LRA enhanced intracellular antioxidant enzyme, superoxide dismutase (SOD), catalase (CAT) activities and markedly reduced malondialdehyde (MDA), total cholesterol (TC), and triglycerides (TG) levels under high-fat stress, demonstrating favorable in vivo lipid-lowering capacity, and LRA exhibited superior performance relative to LRW. Gene sequencing results suggested that several Kyoto Encyclopedia of Genes and Genomes (KEGG) pathways including glycine, serine and threonine metabolism, alcoholic liver disease, peroxisome proliferator-activated receptor (PPAR) signaling pathway, galactose metabolism, etc., may be associated with the lipid-lowering effect of LRA, while LRW may be indirectly associated with lipid-lowering via phenylalanine and tyrosine metabolism pathways. This study provided a theoretical basis for lotus root polysaccharides in lipid-lowering application.

Keywords: lotus root polysaccharide; lipid-lowering activity; *Drosophila*; transcriptome analysis

Check for updates

Academic Editor: Andriy Synytsya

Received: 23 July 2026
Revised: 13 September 2026
Accepted: 18 September 2026
Published: 20 September 2026

Copyright: © 2026 by the authors. Licensee MDPI, Basel, Switzerland. This article is an open access article distributed under the terms and conditions of the Creative Commons Attribution (CC BY) license.

1. Introduction

Long-term excessive intake of high-fat foods is a major risk factor for hyperlipidemia, which further induces a series of metabolic disorders and chronic diseases, including atherosclerosis, hypertension, type 2 diabetes, and obesity [1]. Typically, high-fat

(HF) diet triggered lipid metabolism dysfunction is characterized by elevated levels of total cholesterol (TC), triglycerides (TG), and low-density lipoprotein cholesterol (LDL-C) in vivo [2]. At present, the disorder of lipid metabolism caused by high-fat diet has become one of the serious public health problems and caused serious economic and social burden worldwide [3,4]. Clinically, synthetic lipid-lowering agents (statins, bile acid-binding resins, niacin, fibrates, omega-3 polyunsaturated fatty acids) are used for dyslipidemia management. However, treatment costs and variable adverse reactions may limit therapeutic benefits in certain patients. Therefore, it is imperative to explore safe, efficient, and low-toxic natural lipid-lowering active substances for the prevention and auxiliary treatment of hyperlipidemia.

In recent years, food-derived natural bioactive compounds, particularly plant polysaccharides and polyphenols, have attracted extensive research attention due to their favorable lipid-regulating effects and high safety profiles [5,6]. Mounting mechanistic evidence indicates that plant polysaccharides exert hypolipidemic functions through multiple interconnected pathways, including suppressing de novo lipogenesis, promoting fatty acid β-oxidation, alleviating oxidative stress, and modulating lipid-related transcriptional networks [7,8]. Lotus root (Nelumbo nucifera Gaertn) is a traditional edible and medicinal aquatic vegetable with rich nutritional value and abundant functional ingredients, including polysaccharides, polyphenols, flavonoids, etc. [9]. As the core bioactive component of lotus root, lotus root polysaccharides (LRPs) possess multiple pharmacological activities, including anti-diabetes, anti-osteoporosis, antioxidation, anti-inflammatory, anti-tumor, immunomodulatory and regulation of gut microbiota, demonstrating promising application potential as functional food additives and health care raw materials [10,11]. Recent in vivo investigations have further confirmed that lotus root-derived bioactive fractions could mitigate high-fat-provoked lipid accumulation via AMPK-mediated lipolysis–lipogenesis balance, yet most available studies focused on mixed extracts or polysaccharide-polyphenol complexes, and structure-activity relationships of purified individual LRP fractions remain insufficiently characterized [9]. Our previous research successfully isolated and purified two LRP fractions, namely water-extracted LRW and alkali-extracted LRA. Structural characterization confirmed that the molecular weights of LRW and LRA were 2.464×10^5 Da and 1.727×10^5 Da, respectively. Both fractions shared a main backbone of →4)-α-D-Glcp-(1→ with a small number of →6)-α-D-Glcp-(1→ branched chains [12]. In vitro studies suggested that these two lotus root polysaccharides showed good lipid-lowering activity. Nevertheless, the in vivo lipid-regulating activity and underlying molecular mechanisms of the two LRP fractions remain unclear, which greatly restricts their further development and utilization. Hence, systematic exploration of their in vivo lipid-lowering effects and mechanisms is urgently required.

Drosophila melanogaster with the characteristics of a short life cycle has a high homology of genes related to human diseases (up to 74%), and a similar energy metabolism balance mechanism to that of mammals, which has gradually become an effective biological model for studying metabolic diseases [13,14]. Multiple recent studies have validated the feasibility of the *Drosophila* HF model for lipid metabolism research. For instance, He et al. demonstrated that hijiki polysaccharides could alleviate high-glucose-induced lipid accumulation and developmental abnormalities in *Drosophila* by suppressing the transcription of Srebp and Fas, activating PPAR and Cpt1 activities, and promoting fatty acid β-oxidation [15]. Meanwhile, accumulating studies have established mature detection systems and evaluation criteria for assessing natural compound-mediated metabolic regulation and antioxidant defense in *Drosophila* models [16]. Benefiting from well-annotated genome information, RNA-seq transcriptome analysis in *Drosophila* enables high-throughput screening of core lipid-regulatory genes and signaling cascades, providing cost-effective clues

for deciphering natural polysaccharide action modes prior to rodent verification [17,18]. Therefore, *Drosophila* is becoming more widely used as a model for lipid-lowering research in vivo.

Therefore, in this study, HF-induced hyperlipidemia *Drosophila* model was constructed to evaluate the in vivo lipid-lowering effects of LRW and LRA. Multiple physiological and biochemical indices were determined, including food intake, lifespan, antioxidant enzyme activities, malondialdehyde content, as well as TC and TG levels, to comprehensively assess the regulatory effects of LRW and LRA on HF-induced lipid metabolism disorder. Furthermore, transcriptome sequencing was performed to screen key differentially expressed genes and pivotal signaling pathways involved in LRP-mediated lipid regulation, to preliminarily elucidate the underlying molecular mechanisms. This study aimed to provide in vivo phenotypic and transcriptomic evidence, and further fill the knowledge gap from our previous in vitro work, offering a theoretical basis for the development and application of lotus root polysaccharide as natural lipid-lowering functional ingredients.

2. Materials and Methods

2.1. Materials and Reagents

α-amylase (*Bacillus subtilis*, enzyme activity 4000 U/g) and brilliant blue were purchased from Yuanye Biotechnology Co., Ltd. (Shanghai, China). Corn flour and brown sugar were sourced from a local market in Wuhan, China. Agar was obtained from Saiguo Biotechnology Co., Ltd. (Guangzhou, China). 30% Hydrogen Peroxide was purchased from Guanghua Technology Co., Ltd. (Shaoguan, China). High-activity dry yeast was purchased from Anqi Yeast Co., Ltd. (Yichang, China). Propionic acid was supplied by Sinopharm Chemical Reagent Co., Ltd. (Shanghai, China). Superoxide dismutase (SOD) assay kits, catalase (CAT) assay kits, malondialdehyde (MDA) assay kits, TC and TG assay kits were purchased from Nanjing Jiancheng Bioengineering Research Co., Ltd. (Nanjing, China). Carbon dioxide (with a purity of ≥99.9%) was obtained from Minghui Gas Technology Co., Ltd. (Wuhan, China).

2.2. Preparation of Lotus Root Polysaccharide

The extraction of LRW and LRA from lotus root were carried out in accordance with the method established in our previous research [19]. In detail, fresh lotus root (Elian 5, Wuhan Jinshui Qiliang Agricultural Byproducts Co., Ltd., Wuhan, China) was washed, sliced, dried at 65 °C for 12 h, ground in a high-speed universal grinder for 2~4 min, and sieved through a 100-mesh sieve to obtain lotus root powder. For LRW preparation, lotus root powder was homogenized in ultrapure water at a solid/liquid ratio of 1:10 (g/mL). The mixture was treated with 0.2% α-amylase at 55 °C for 4 h for complete starch removal, confirmed by a negative iodine test, followed by 2 h incubation at 90 °C to inactivate the enzyme. After cooling and centrifugation (4500 r/min, 10 min), the supernatant was concentrated and subjected to preliminary precipitation with 30% ethanol at 4 °C for 3 h. The resulting supernatant was deproteinized by overnight stirring with 717 anion-exchange resin. After filtration to remove the resin, the solution was precipitated with 75% ethanol at 4 °C overnight. The harvested precipitate was redissolved and dialyzed with a 1000 Da MWCO membrane against ultrapure water for 3 days and freeze-dried to obtain purified LRW.

For LRA extraction, the dried residue after water extraction was used as the raw material. Referring to the optimized alkaline extraction protocol reported previously [19], the residue was dispersed in 0.04 mol/L NaOH solution at a solid/liquid ratio of 1:16 (g/mL), incubated at 57 °C for 1.3 h, and centrifuged to collect the supernatant. The supernatant was neutralized to pH 7.0 with HCl, and then purified through the same procedures as LRW,

including graded ethanol precipitation, resin deproteinization, dialysis and lyophilization, yielding purified LRA.

2.3. Drosophila Culture and Preparation of Medium

Drosophila culture. *Drosophila melanogaster* w^{1118} were cultivated in an incubator at 26 ± 0.1 °C with a relative humidity of 70% and under a 12 h light/dark cycle.

Preparation of medium. Two types of diet were prepared for the experiment to examine the lipid-lowering effect of LRW and LRA in *Drosophila*. Basal medium was prepared by dissolving 30 g corn, 30 g brown sugar, 2 g yeast, 2 g agar and 2 mL propionic acid in 300 mL hot water and dispersed fully, finally cooled to form. The preparation of high-fat medium was to add 10% lard on the basis of the basic medium, and other conditions remain unchanged according to the reporter method [20]. For the medium in experimental group, lotus root polysaccharide (LRW and LRA) solution with different concentration (1, 5, 10 mg/mL) were added to the surface of the prepared high-fat medium respectively, which were named as low, medium and high doses of LRW experimental group (LRW-L, LRW-M, LRW-H) and LRA experimental group (LRA-L, LRA-M, LRA-H). Filter-sterilized polysaccharide solutions were evenly pipetted onto the fully solidified medium surface. After droplet spreading, vials were placed horizontally at 26 °C for 30 min to allow complete surface absorption before adding flies. The medium vials were kept horizontal during the whole 3-day feeding cycle to avoid liquid flow-induced concentration deviation, ensuring relatively homogeneous polysaccharide distribution for consistent fly exposure. Fresh medium was replaced every three days during the experiment. It should be noted that the medium-surface doses for the *Drosophila* feeding model cannot be directly translated to human physiological equivalent doses, which were used solely for bioactivity evaluation in this study for *Drosophila*.

2.4. Determination of Drosophila Appetite

The 3-day-old male and female *Drosophila* were artificially separated and subjected to 24 h of starvation treatment. Subsequently, male and female *Drosophila* were fed with basal medium and high-fat medium containing 0.5% (*w*/*w*) acidic blue dye, respectively. After 4 h of dark feeding, the *Drosophila* were anesthetized with CO, fully homogenized in 1 mL PBS using a homogenizer, and centrifuged at 4500 r/min for 5 min. The supernatant was collected, and the absorbance value at 625 nm was determined. The relative food consumption of *Drosophila* was quantified and reflected by the absorbance difference of acidic blue dye, and the calculation was performed using Equation (1).

$$\mathrm{OD} = A_a - A_b \quad (1)$$

where the calculated OD value represents the relative food intake of *Drosophila*; A_a is the absorbance of homogenate supernatant from flies fed dye-supplemented experimental media; A_b represents the background absorbance from flies fed basal medium without acidic blue dye, serving as biological blank to correct intrinsic fly-derived absorbance.

2.5. Determination the Lifespan of Drosophila

The lifespan of *Drosophila* was measured referring to the reported method [21]. Three-day-old *Drosophila* from the same batch were collected and the males and females were separated, then randomly assigned into eight groups: the normal group, high-fat group, LRA-L group, LRA-M group, LRA-H group, LRW-L group, LRW-M group, and LRW-H group. Each group contained 200 flies, distributed across 10 culture tubes. Male and female flies were assayed separately. Flies were cultured under the conditions described in Section 2.3, and the culture medium was refreshed every 3 days. The number of surviving

flies was recorded until all flies died, and the survival curve was constructed based on the recorded data. The data were subsequently analyzed with GraphPad Prism (version 9.0) and plotted as a Kaplan-Meier survival plot after the treatment period. Specifically, the mean lifespan was calculated as the total lifespan of all individual flies in each group divided by the total number of flies in the corresponding group; the median lifespan was defined as the time point at which half of the flies in each group had died, while the maximum lifespan was determined as the average lifespan of the longest-lived 10% of flies in each group [22].

2.6. Determination of Sod, Cat, Mda, Tc and Tg in Drosophila

According to the culture conditions in 2.3 and 2.5, male and female *Drosophila* were separately cultured for 10, 20, and 40 days. For sample collection, each group was set up with three independent biological replicates, and each biological replicate contained 20 age- and gender-consistent flies. After starvation treatment for 2 h, the *Drosophila* were anesthetized and weighed, and the pre-cooled saline was added at a ratio of 1:49 (g/mL) of the *D. melanogaster* body weight at 4 °C, and then centrifuged at 4500 r/min for 15 min under 4 °C. After centrifugation, the supernatant was taken to determine the CAT and SOD level, TC and TG contents, as well as the MDA activity by using the assay kit.

2.7. Transcriptome Sequencing Analysis

For transcriptome sequencing, 20-day-old female *Drosophila* treated with high-dose (10 mg/mL) LRW and LRA were sampled. Total RNA was isolated from different groups of *Drosophila* (Control, HF, LRA, LRW) by using TRIzol Reagent (Invitrogen, Carlsbad, CA, USA) following the manufacturer's instructions. The mRNA was purified, and cDNA synthesis, end repair, 'A' nucleotide addition, adapter ligation and amplification were performed successively. After denaturation, single-stranded PCR was performed for circling and replication by rolling-cycle amplification, followed by loading into patterned nanoarrays using high-strength DNA nanochip technology and sequencing by combinatorial probe-anchor synthesis (cPAS). RNA libraries were constructed using the VAHTS Universal V6 RNA-seq Library Prep Kit for Illumina (Vazyme, Nanjing, Jiangsu, China). High-throughput transcriptome sequencing was performed on the Illumina NovaSeq 6000 platform with a paired-end 150 bp (PE150) read length. The average sequencing depth was 6 G clean reads per sample, and Q30 value was guaranteed above 90%. All RNA extraction, library construction and sequencing experiments were completed in a single independent batch to eliminate technical variation, and thus no additional batch-effect correction was performed in the subsequent bioinformatics analysis. In addition, only female *Drosophila* were used for transcriptome sequencing, which completely excluded the interference of sex differences on gene expression profiles. For differential gene expression analysis, the NOISeq method was adopted with unified and standardized screening parameters. Genes with fold change ≥ 2 and adjusted Q-value < 0.05 after rigorous multiple-testing correction were identified as differentially expressed genes (DEGs). For KEGG pathway enrichment analysis, Q-value was calculated based on hypergeometric distribution, and the Benjamini–Hochberg procedure was applied for multiple-testing correction to obtain FDR-adjusted Q-values. Pathways with Q-value < 0.05 were considered significantly enriched.

2.8. Statistical Analysis

Data were presented as the mean ± standard deviation (SD) of at least three independent biological replicates with each replicate using separate *Drosophila* cohorts, and each biological replicate included three technical replicates. All statistical analyses were performed using SPSS software (version 26.0). Prior to parametric statistical testing, Shapiro-Wilk test and Levene's test were performed to verify data normality and homogeneity of variance,

respectively. Student's *t*-test was used for pairwise comparisons between two groups. For multi-group comparisons, the Kruskal-Wallis H test was adopted for overall testing, followed by Dunn's post hoc test with Bonferroni correction for pairwise comparisons. This non-parametric pipeline was chosen because some datasets exhibited uneven variance and slight non-normal distribution, which is suitable for *Drosophila* physiological data. The transcriptome analysis in this study was performed using the BGI Online System (BGI Genomics, Shenzhen, China).

3. Results and Discussion

3.1. Extraction and Characterization of Lotus Root Polysaccharides

LRW and LRA were extracted via hot water and dilute alkali method, respectively. Our prior study comprehensively investigated their fundamental composition and structural characteristics [12], with key findings consolidated in Table 1. The extraction yields of LRW and LRA obtained by the above methods were 1.68% and 13.07%, respectively. LRW contained considerably higher total sugar (96.83%) than LRA (73.66%), whereas protein levels were relatively low in both samples (1.52% and 2.50%). LRW mainly consisted of glucose, accompanied by trace amounts of rhamnose, galactose and arabinose with molar ratios of 1:0.01:0.007:0.039. In contrast, LRA displayed a more diverse monosaccharide profile, comprising glucose, mannose, rhamnose, galactose and arabinose, with molar ratios of 1:0.01:0.016:0.107:0.025. The molecular weights of LRW and LRA were 2.464×10^5 Da and 1.727×10^5 Da, respectively. Combined with monosaccharide composition analysis, methylation analysis and nuclear magnetic resonance spectroscopy, it can be concluded that LRW and LRA shared a similar main structure: →4)-α-D-Glcp-(1→ branched with →6)-α-D-Glcp-(1→. LRW and LRA differed primarily in monosaccharide composition and molecular weight, which could be the critical contributors to their divergent bioactivities.

Table 1. Basic properties and structure of the LRW and LRA polysaccharides from lotus root [12].

Items	LRW	LRA
Yield (%)	1.68	13.07
Total sugar content (%)	96.83	73.66
Protein content (%)	1.52	2.50
Monosaccharide composition	Glc:Rha:Gal:Ara ≈ 1:0.01:0.007:0.039	Glc:Man:Rha:Gal:Ara ≈ 1:0.01:0.016:0.107:0.025
Molecular weight	2.464×10^5 Da	1.727×10^5 Da
Main structure	→4)-α-D-Glcp-(1→ branched with →6)-α-D-Glcp-(1→	→4)-α-D-Glcp-(1→ branched with →6)-α-D-Glcp-(1→

3.2. Effect of Lotus Root Polysaccharides on the Appetite of D. melanogaster

To clarify whether lotus root polysaccharides affect the feeding behavior and appetite of *D. melanogaster*, a dye labeling method was applied to determine the food intake of flies under different dietary conditions [23]. Polysaccharide concentrations (1, 5, 10 mg/mL) were selected from our preliminary dose-screening assays and published *Drosophila* polysaccharide studies [24]. This gradient spans low-, medium- and high-effect doses and avoids overly high concentrations that could alter medium physical properties. As shown in Figure 1, comparative analysis of feeding volume among groups showed significant gender differences in the appetite response of *Drosophila* to high-fat diet stimulation. Specifically, compared with the normal diet group, female *Drosophila* exhibited a markedly increased food intake after switching to a high-fat diet, whereas male flies showed no significant alteration in food consumption under high-fat feeding conditions. Subsequent polysaccharide intervention experiments further suggested that no significant difference in food intake

was observed between the HF group and the LRW- or LRA-supplemented HF groups in either male or female *Drosophila* ($p > 0.05$). These results indicated that LRW and LRA had no obvious effect on the feeding preference and food intake of *Drosophila*, eliminating the interference of differential food consumption on physiological and biochemical indicators in subsequent experiments. Considering the gender-based discrepancy in feeding response to high-fat diet, both male and female *Drosophila* were included in the follow-up experiments.

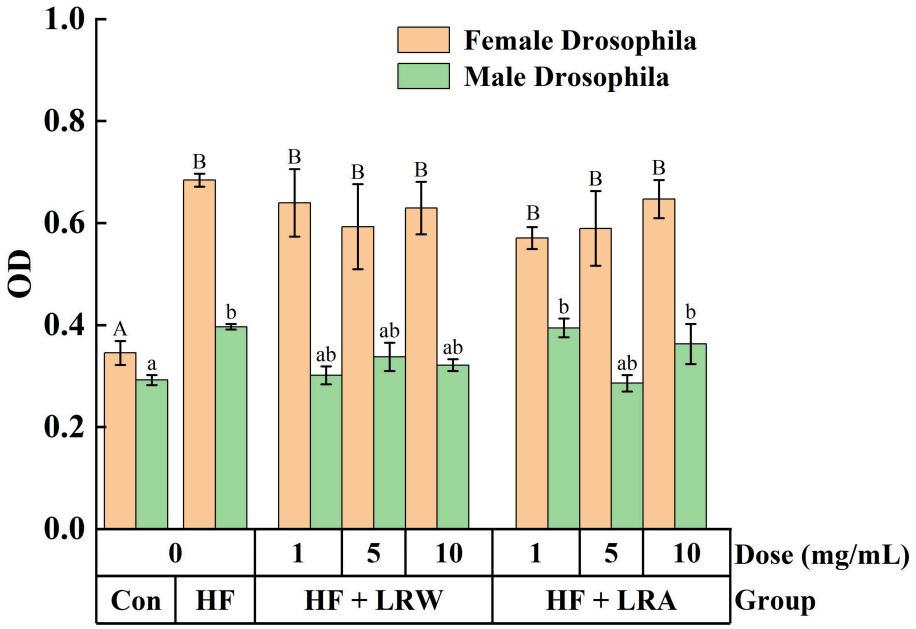

Figure 1. Effect of two lotus root polysaccharides on appetite of *Drosophila melanogaster*. Data are expressed as mean ± SD, $n = 5$ independent biological replicates (separate fly cohorts). Statistical analyses were performed using the non-parametric Kruskal-Wallis test followed by Dunn's post hoc test with Bonferroni correction for multiple-group comparisons. Different capital letters indicate significant differences ($p < 0.05$) among female groups. Different lowercase letters indicate significant differences ($p < 0.05$) among male groups.

3.3. Effect of Lotus Root Polysaccharides on the Lifespan of D. melanogaster

With a short life cycle and simple breeding conditions, *Drosophila melanogaster* has been widely applied in aging and lifespan regulation research, and has become a classic model organism for evaluating dietary stress-induced senescence and lifespan changes [25]. Accumulating studies have confirmed that high-fat diet stress can trigger oxidative damage and metabolic disorders in *Drosophila*, thereby accelerating aging progression and shortening lifespan [26,27]. Here, the lifespan regulatory effects of LRW and LRA lotus root polysaccharides on HF-induced male and female *Drosophila* were systematically analyzed based on survival curves and lifespan statistical parameters (Figure 2, Table 2). Consistent with typical HF-induced aging phenotypes, HF feeding significantly shortened the average, median, and maximum lifespan of both female and male *Drosophila* compared with the normal control group ($p < 0.05$), confirming that high-fat nutrition stress successfully induced aging and lifespan decline in flies. For female *Drosophila*, all dosage groups of LRW failed to produce significant lifespan extension in female *Drosophila*. By contrast, LRA supplementation exhibited a dose-dependent lifespan-improving effect. Specifically, medium and high doses of LRA (5 and 10 mg/mL) significantly rescued the HF-induced reduction in average lifespan. The average lifespan of the HF group was 36.87 ± 4.22 days, which was prominently extended to 45.93 ± 3.76 days and 42.20 ± 3.28 days in LRA-M and LRA-H groups, respectively. In addition, LRA-M treatment achieved the optimal longevity effect in female flies, with the maximum lifespan increased by over 4% and the

median lifespan remarkably prolonged from 46.80 ± 3.19 days (HF group) to 53.40 ± 3.50 days. The distinct lifespan disparity between LRA and LRW observed in this study can be reasonably explained by their structural and compositional differences. Consistent with our results, recent structural activity studies of lotus root polysaccharides demonstrated that low-molecular-weight polysaccharides with diversified monosaccharide components exhibit better bioavailability and stronger biological regulatory activity [12].

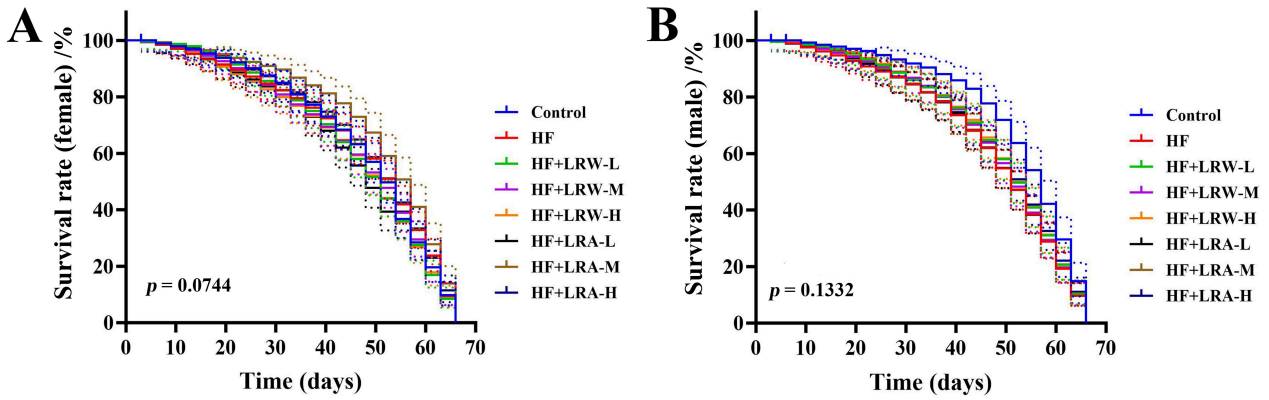

Figure 2. Lifespan curve of *Drosophila melanogaster* ((**A**) female *Drosophila*; (**B**) male *Drosophila*). Data are expressed as mean ± SD, n = 5 independent biological replicates (separate fly cohorts). Survival differences among groups were assessed by Log-rank (Mantel-Cox) test, the p-values represent the overall significance for the whole survival curves. The dotted lines in matching colors indicate error bars for their respective survival curves.

Table 2. Lifespan of *Drosophila* fed a control diet and HF at low, medium, and high doses of LRW and LRA.

Gender	Group	Mean Lifespan (Day)	Median Lifespan (Day)	Maximum Lifespan (Day)
Female *Drosophila*	Control	40.55 ± 2.84 ^{bc}	45.50 ± 2.80 ^{bc}	62.70 ± 0.90 ^{a}
	HF	36.87 ± 4.22 ^{de}	46.80 ± 3.19 ^{bc}	57.60 ± 3.50 ^{bcd}
	HF + LRW-L	33.99 ± 4.10 ^{e}	38.50 ± 4.15 ^{d}	53.25 ± 2.49 ^{d}
	HF + LRW-M	39.56 ± 3.07 ^{cd}	47.00 ± 1.00 ^{abc}	57.75 ± 2.49 ^{bcd}
	HF + LRW-H	35.90 ± 1.81 ^{e}	44.75 ± 1.09 ^{bc}	54.00 ± 4.24 ^{cd}
	HF + LRA-L	34.90 ± 3.25 ^{e}	39.80 ± 5.64 ^{cd}	54.60 ± 3.50 ^{cd}
	HF + LRA-M	45.93 ± 3.76 ^{a}	53.40 ± 3.50 ^{a}	60.60 ± 3.50 ^{ab}
	HF + LRA-H	42.20 ± 3.28 ^{b}	49.00 ± 4.77 ^{ab}	58.20 ± 4.87 ^{abc}
Male *Drosophila*	Control	46.87 ± 3.01 ^{a}	48.89 ± 3.90 ^{a}	61.67 ± 2.89 ^{ab}
	HF	35.82 ± 3.85 ^{c}	41.00 ± 3.52 ^{c}	55.20 ± 1.47 ^{c}
	HF + LRW-L	39.54 ± 1.52 ^{bc}	43.20 ± 1.60 ^{ab}	57.60 ± 1.20 ^{bc}
	HF + LRW-M	37.20 ± 4.39 ^{bc}	39.60 ± 3.98 ^{c}	54.60 ± 2.24 ^{c}
	HF + LRW-H	38.31 ± 1.98 ^{bc}	43.00 ± 0.89 ^{ab}	57.60 ± 2.24 ^{bc}
	HF + LRA-L	41.29 ± 4.71 ^{b}	45.00 ± 5.52 ^{ab}	55.50 ± 3.35 ^{c}
	HF + LRA-M	38.40 ± 2.58 ^{bc}	41.40 ± 3.93 ^{c}	64.20 ± 1.47 ^{a}
	HF + LRA-H	41.20 ± 2.30 ^{b}	45.40 ± 3.44 ^{ab}	61.80 ± 2.40 ^{ab}

Data are presented as mean ± SD, n = 5 independent biological replicates (separate fly cohorts). Statistical analyses were performed using the non-parametric Kruskal-Wallis test followed by Dunn's post hoc test with Bonferroni correction for multiple-group comparisons. Different lowercase letters indicate significant differences ($p < 0.05$) among different groups.

Notably, distinct sexual dimorphism was observed in the lifespan response of *Drosophila* to polysaccharide intervention. In male flies, HF-induced lifespan damage was also evident, with a baseline average lifespan of 35.82 ± 3.85 days in the HF group. Different from females, male flies obtained optimal longevity benefits from low and high

doses (1 and 10 mg/mL) of LRA. LRA-L and LRA-H treatment significantly elevated the average lifespan of HF-fed male flies, reaching 41.29 ± 4.71 days and 41.20 ± 2.30 days, respectively (Table 2). However, all LRW dosages only exerted slight and non-significant improvements on the lifespan of male *Drosophila*. This sex-dependent protective pattern is consistent with previous reports on plant polysaccharide intervention in *Drosophila* metabolic aging, which confirmed that female flies are more sensitive to medium-dose polysaccharide intervention [28].

Mean lifespan, the total lifespan of all flies divided by the total fly number in each group; median lifespan, the time point when half of the flies in each group died; maximum lifespan, the average lifespan of the top 10% longest-lived flies in each group. Data are expressed as mean ± SD, $n = 5$ independent biological replicates (separate fly cohorts). Statistical analyses were performed using the non-parametric Kruskal-Wallis test followed by Dunn's post hoc test with Bonferroni correction for multiple-group comparisons. Different lowercase letters indicate significant differences ($p < 0.05$) among different groups.

3.4. Antioxidant Activity of Lotus Root Polysaccharides in D. melanogaster

Excessive lipid intake disrupts in vivo energy homeostasis, induces excessive accumulation of reactive oxygen species (ROS), suppresses endogenous antioxidant enzyme activity, and triggers lipid peroxidation, which further increases MDA content and ultimately causes severe oxidative stress. SOD and CAT are core antioxidant enzymes responsible for scavenging intracellular oxygen free radicals, while MDA is a key end-product of lipid peroxidation; these three indicators are widely adopted to comprehensively evaluate the in vivo antioxidant capacity and oxidative damage level of organisms [29,30]. To explore the antioxidant regulatory effects of LRW and LRA under high-fat dietary stress, the activities of MDA, SOD and CAT content of male and female *Drosophila* at 10, 20 and 40 days were determined (Figure 3). *Drosophila* at 10, 20 and 40 days corresponds to young, middle-aged and aged adult stage, enabling monitoring of dynamic antioxidant changes across adulthood.

MDA quantification (Figure 3A,B) indicated that HF feeding significantly increased MDA accumulation in *Drosophila* at young, middle-aged, and aged stages in both sexes ($p < 0.05$), indicating persistent high-fat-induced lipid peroxidation throughout the lifespan. Consistent with natural senescence characteristics, both blank control and HF groups exhibited elevated basal MDA levels in aged flies (40-day), suggesting that MDA accumulation was closely aggravated by aging progression. Regardless of gender, the inhibitory effects of LRW and LRA on HF-induced MDA overproduction presented an obvious dose-dependent pattern: low-dose polysaccharides (1 mg/mL) showed weak MDA scavenging ability, while medium and high doses (5 and 10 mg/mL) exerted significantly stronger inhibitory efficacy. In female *Drosophila*, medium and high doses of LRA prominently reduced MDA content and restored lipid peroxidation status close to the normal physiological range. In male flies, medium and high doses of LRW and LRA also effectively alleviated HF-triggered MDA accumulation. Importantly, although aged flies exhibited higher baseline oxidative damage, medium- and high-dose LRW and LRA still maintained potent MDA inhibitory effects in the aged stage, demonstrating reliable anti-lipid peroxidation capacity even under aging superimposed with high-fat metabolic stress.

SOD and CAT exhibited highly consistent variation trends in response to HF and polysaccharide intervention (Figure 3C–F). HF significantly inhibited the activities of both antioxidant enzymes in *Drosophila* ($p < 0.05$), confirming that high-fat stress profoundly impaired endogenous antioxidant defense [31,32]. However, LRW and LRA showed distinct antioxidant characteristics regarding gender and age regulation. In female *Drosophila*, LRA produced prominent dose-dependent upregulation of both SOD and CAT activities across

all developmental stages, with high-dose LRA (LRA-H) presenting the optimal efficacy (Figure 3C,E). Specifically, LRA-H exhibited the most potent antioxidant capacity, which significantly elevated SOD activity by 16.4%, 20.3%, and 13.11% at 10, 20 and 40 days, respectively, restoring the antioxidant level even higher than that of the blank group. In contrast, LRW had limited antioxidant effects in female flies, and low-dose LRW failed to recover HF-induced enzymatic inhibition. In male *Drosophila*, HF significantly reduced SOD and CAT activities at young and middle-aged stages (10 and 20 days), whereas no obvious damage was observed in aged flies (Figure 3D,F). LRA exhibited stable and universal protective effects in males, effectively restoring SOD and CAT activities throughout young, middle-aged, and aged stages. By comparison, the antioxidant performance of LRW was strongly restricted by age: LRW only improved antioxidant enzyme activities in young and middle-aged male flies and showed no rehabilitative effect in young males at 10 days.

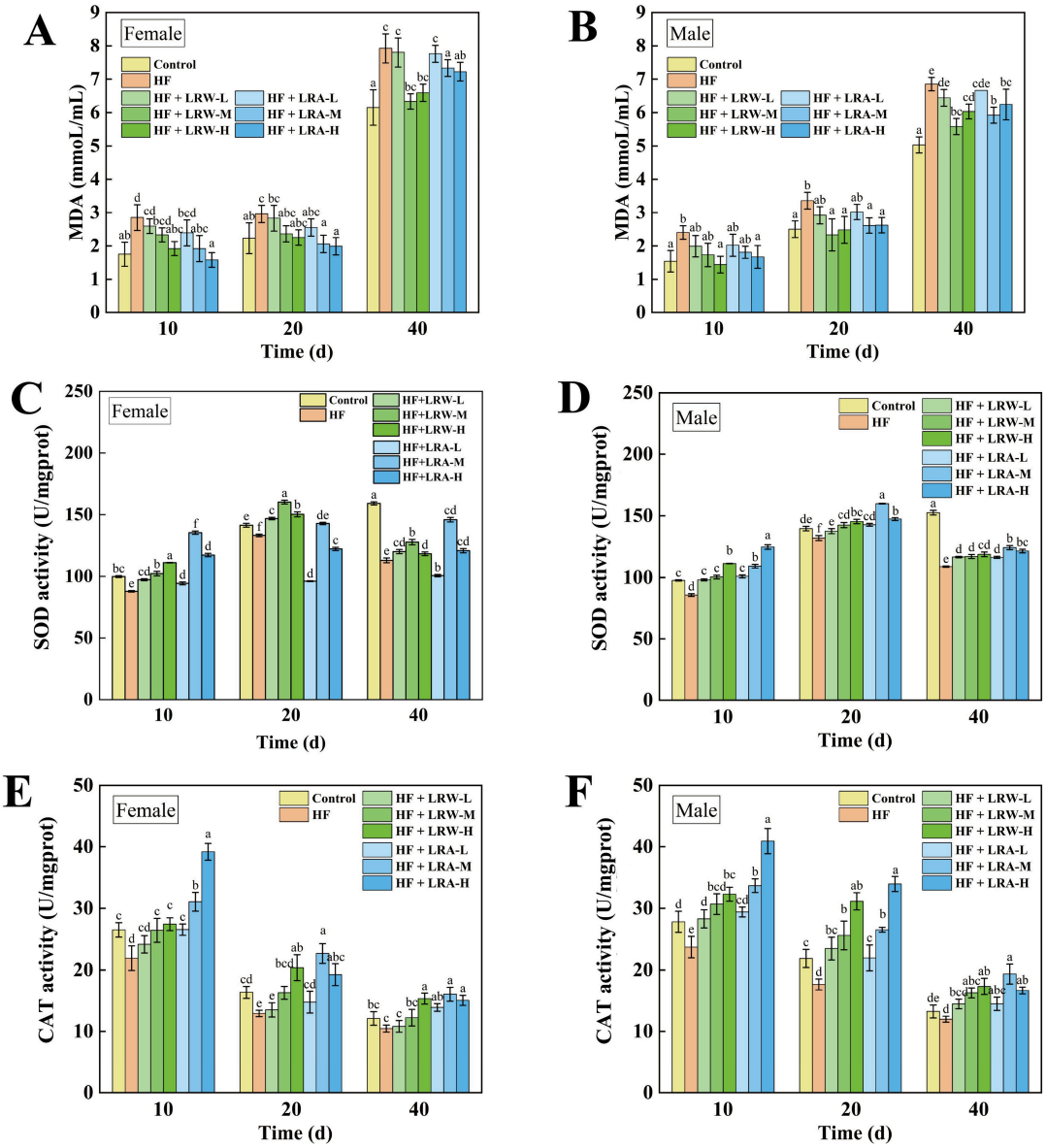

Figure 3. The MDA level ((**A**) female; (**B**) male), the activity of SOD ((**C**) female; (**D**) male), and the CAT activity ((**E**) female; (**F**) male) in *Drosophila* under high-fat diet stress with LRW and LRA interventions at 10, 20 and 40 days. Data are expressed as mean ± SD, $n = 4$ independent biological replicates (separate fly cohorts). Statistical analyses were performed using the non-parametric Kruskal-Wallis test followed by Dunn's post hoc test with Bonferroni correction for multiple-group comparisons. Different lowercase letters indicate significant differences ($p < 0.05$) among different groups.

The significant difference in antioxidant activity between LRA and LRW was likely primarily attributable to their inherent structural differences, which was consistent with current polysaccharide structure–activity relationship theories. Structurally, LRA has a lower molecular weight and richer monosaccharide composition (containing mannose, galactose, rhamnose, and arabinose), which can provide more active sites for ROS scavenging and antioxidant enzyme activation. Existing studies have confirmed that hetero-polysaccharides with diversified monosaccharide components possess stronger antioxidant and metabolic regulatory activities than homogeneous glucan polysaccharides [33,34]. In comparison, LRW is a high-purity homogeneous glucan with a larger molecular weight and single sugar composition, resulting in poor flexibility of molecular chain structure and fewer active functional sites, thus limiting its antioxidant regulatory range and stability. Meanwhile, the slightly higher protein content of LRA (2.5%) than LRW (1.52%) also contributes to its enhanced antioxidant performance, as trace bound protein can synergistically improve the free radical scavenging ability of polysaccharides [35]. Collectively, LRA exhibited antioxidant capacity with sex- and age-dependent differences. Its effects were less pronounced in aged male flies than in females at certain time points, while LRW exerted weaker effects with obvious gender and age limitations.

3.5. Lipid-Lowering Activity of Lotus Root Polysaccharides in D. melanogaster

Long-term high-fat diet intake severely disrupts in vivo lipid metabolism homeostasis, causing excessive accumulation of total TC and TG. Abnormally elevated TC and TG levels are core manifestations of dyslipidemia, which can trigger lipid metabolic disorders, aggravate in vivo metabolic stress, accelerate senescence progression, and further induce a series of chronic metabolic and cardiovascular diseases [36,37]. To further explore whether LRW and LRA could alleviate HF-induced lipid metabolic damage, the TC and TG levels of female and male *Drosophila* of different age groups (10 d, 20 d, 40 d) of *Drosophila* were determined (Figure 4). The lipid-regulating effects of LRW and LRA were markedly dependent on polysaccharide dosage, sex, and age of flies. For young female flies (10-day), low-dose polysaccharides (5 mg/mL) failed to significantly reduce TC accumulation, whereas low-dose intervention obviously improved hyperlipidemia symptoms in young male flies, showing distinct sexual dimorphism in the early response to polysaccharide treatment (Figure 4A,B). In middle-aged (20-day) and aged (40-day) male and female *Drosophila*, medium and high doses of LRW and LRA (5 and 10 mg/mL) exerted prominent TC-lowering effects. Specifically, LRA-H achieved optimal TC reduction in 20-day flies, while LRA-M and LRW-H showed the best efficacy in aged (40-day) *Drosophila*, which could restore HF-induced elevated TC levels close to the normal physiological range. These results indicated that low-dose lotus root polysaccharides had limited lipid-lowering effects, whereas medium and high concentrations possessed stable and effective TC regulatory capacity, and could reverse high-fat-induced cholesterol metabolic disorders in middle and late developmental stages.

HF exposure significantly increased TG levels in *Drosophila* at young, middle-aged, and aged stages ($p < 0.05$), and TG accumulation was further aggravated with aging. Notably, under the same high-fat culture conditions, female flies showed more severe TG overaccumulation than males, indicating that female individuals were more susceptible to high-fat lipid metabolic injury. Consistent with the variation trend of TC, both LRW and LRA exerted significant dose-dependent inhibitory effects on HF-induced TG elevation, with medium- and high-dose polysaccharides displaying far stronger TG-lowering efficacy than low-dose groups (Figure 4C,D). In addition, comprehensive comparison revealed that LRA possessed more prominent TG regulatory capacity than LRW throughout all developmental stages. Specifically, medium- and high-dose LRA effectively alleviated HF-triggered TG

accumulation in flies of different sexes and ages. By contrast, only high-dose LRW exerted significant TG-lowering activity in aged flies. Even in aged flies with naturally elevated TG baseline, medium- and high-dose LRA still maintained stable and superior lipid-lowering performance, further verifying its advantages in anti-hyperlipidemic function.

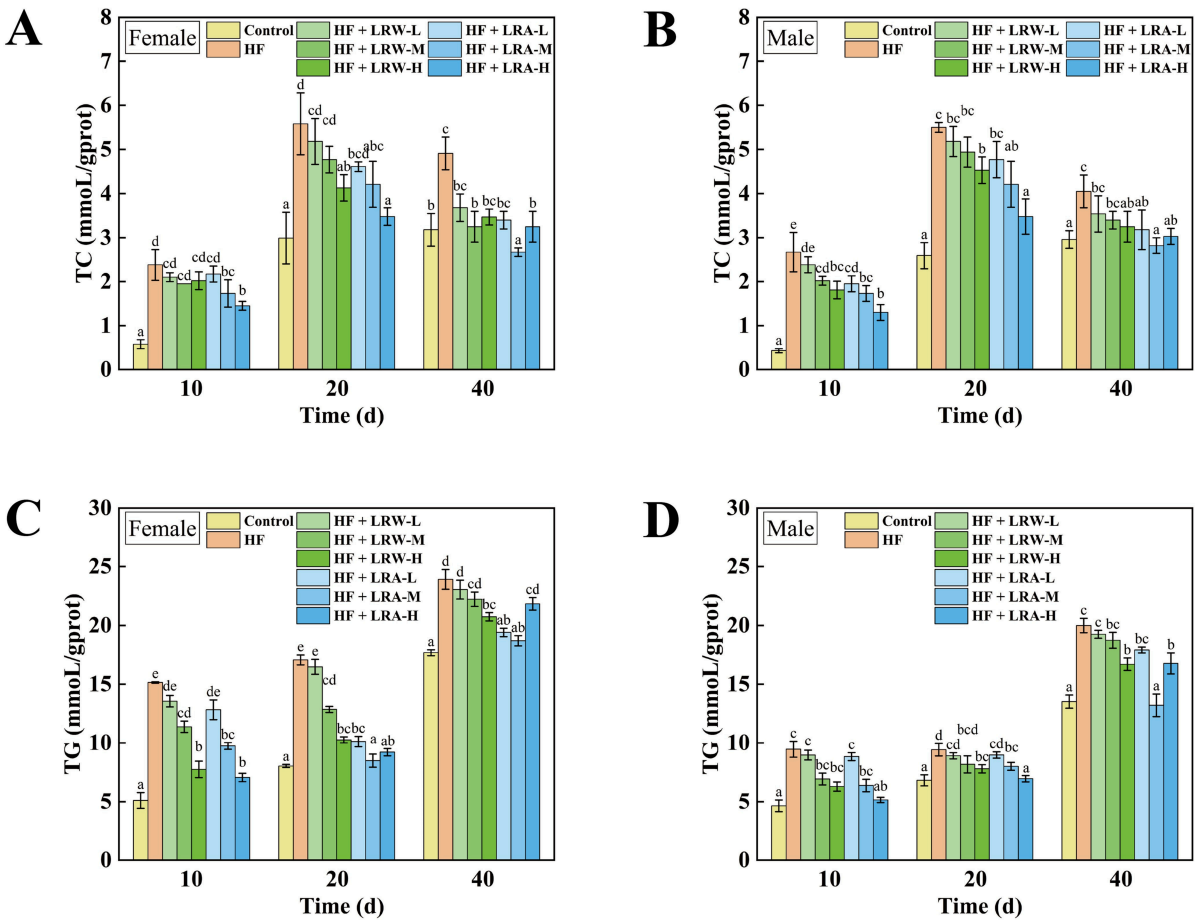

Figure 4. The level of TC ((**A**) female; (**B**) male) and TG ((**C**) female; (**D**) male) in *Drosophila* under high-fat diet stress with LRW and LRA interventions at 10, 20 and 40 days. Data are expressed as mean ± SD, $n = 4$ independent biological replicates (separate fly cohorts). Statistical analyses were performed using the non-parametric Kruskal-Wallis test followed by Dunn's post hoc test with Bonferroni correction for multiple-group comparisons. Different lowercase letters indicate significant differences ($p < 0.05$) among different groups.

In brief, both LRW and LRA dose-dependently alleviated HF-induced oxidative stress and lipid metabolism disorders in *Drosophila*. Medium- and high-dose polysaccharides effectively recovered decreased SOD and CAT activities, reduced excessive MDA accumulation, and suppressed abnormal elevation of TC and TG levels. Moreover, female flies and aged individuals were more susceptible to HF-induced metabolic damage. Compared with LRW, LRA exhibited more stable and superior protective effects against oxidative injury and dyslipidemia across different genders and developmental stages, while LRW showed obvious age-dependent limitations. The consistent superiority of LRA over LRW in lipid-lowering activity is fundamentally attributed to their structural differences, which well explains the structure–activity relationship of lotus root polysaccharides in lipid metabolism regulation. Previous studies have proven that polysaccharides containing galactose, mannose and rhamnose can effectively activate lipid catabolic pathways and inhibit lipogenic gene expression [38,39]. The rich galactose and mannose components in LRA are key active groups for lipid regulation, while LRW is almost purely composed of

glucose with extremely few heterogeneous monosaccharides, resulting in a single regulatory pathway and weak lipid-lowering effect. In summary, the lower molecular weight and diversified monosaccharide composition of LRA are the core structural basis for its superior anti-aging, antioxidant and lipid-lowering activities compared with LRW in HF-induced *Drosophila* model.

3.6. Effect of Lotus Root Polysaccharides on Transcriptional Profiles in D. melanogaster

3.6.1. Analysis of Degs and Functional Annotation of Kegg Pathways

To further reveal the underlying molecular mechanisms by which LRW and LRA alleviated high-fat diet-induced oxidative stress and lipid metabolic disorders, transcriptome sequencing was performed to screen differentially expressed genes (DEGs) and characterize transcriptional regulatory profiles in *Drosophila* under different treatments. Combined with the phenotypic and biochemical results above, the key functional genes and signaling pathways involved in lipid metabolism and oxidative stress response were further analyzed to clarify the intrinsic regulatory differences between the two lotus root polysaccharides. Based on comprehensive analysis of lifespan, antioxidant and lipid-lowering phenotypes, female flies showed more evident biological responses and the high-dose treatment yielded the best effects. Thus 20-day-old female *Drosophila* treated with high dose (10 mg/mL) were selected to characterize transcriptional regulatory responses under polysaccharide intervention. As summarized in Table 3, clean reads of 44.96 ± 0.35, 45.40 ± 0.07, 45.17 ± 0.07, and 45.00 ± 0.13 million were obtained from the Control, HF, HF + LRW, and HF + LRA groups, respectively. All samples exhibited a mapping rate of over 94%, demonstrating that the sequencing quantity and quality were reliable and sufficient for subsequent bioinformatic analysis.

Table 3. Summary of RNA-Seq data quality and mapping statistics.

Sample Name	Total Raw Reads (M)	Total Clean Reads (M)	Total Clean Bases (Gb)	Clean Reads Q20 (%)	Clean Reads Q30 (%)	Clean Reads Ratio (%)
Control-1	47.19	44.49	6.67	97.78	92.53	94.28
Control-2	47.19	45.31	6.8	98.55	95.09	96.03
Control-3	47.19	45.08	6.76	97.78	92.48	95.55
HF-1	47.19	45.44	6.82	97.83	92.66	96.31
HF-2	47.19	45.3	6.79	97.86	92.78	96
HF-3	47.19	45.45	6.82	97.23	90.77	96.33
HF + LRW-1	47.19	44.81	6.72	97.97	93.22	94.97
HF + LRW-2	47.19	45.1	6.77	97.75	92.41	95.58
HF + LRW-3	47.19	45.09	6.76	97.81	92.65	95.56
HF + LRA-1	47.19	45.08	6.76	97.89	92.87	95.53
HF + LRA-2	47.19	45.25	6.79	97.6	91.89	95.91
HF + LRA-3	47.19	45.18	6.78	97.92	92.97	95.76

Multiple statistical analyses were performed to clarify the transcriptional differences among groups, including principal component analysis (PCA), differential gene screening, and Kyoto Encyclopedia of Genes and Genomes (KEGG) functional enrichment analysis. PCA was applied to evaluate the overall transcriptional similarity and sample clustering patterns across different treatment groups. The PCA results (Figure 5A) revealed obvious transcriptional separation between the control and HF groups, indicating that HF treatment induced significant genome-wide transcriptional alterations in *Drosophila*. Both the HF + LRW and HF + LRA groups exhibited closer clustering with the HF group rather than the control group, while distinct transcriptional differences were observed between polysaccharide intervention and model groups.

Volcano plots were generated to visualize the significantly differentially expressed genes (DEGs) induced by LRW and LRA intervention (Figure 5B–D). DEG screening results showed that a total of 146 DEGs were identified in the HF + LRW group compared with the HF group, consisting of 24 significantly upregulated genes and 122 significantly downregulated genes (Figure 5E). By comparison, the HF + LRA group yielded 349 DEGs, including 174 upregulated and 175 downregulated genes (Figure 5F). Venn diagram analysis further screened the common regulatory DEGs among groups, and a total of 40 co-expressed DEGs were shared by LRW and LRA intervention groups (Figure 5G), indicating partial consistent transcriptional regulatory patterns between the two polysaccharides.

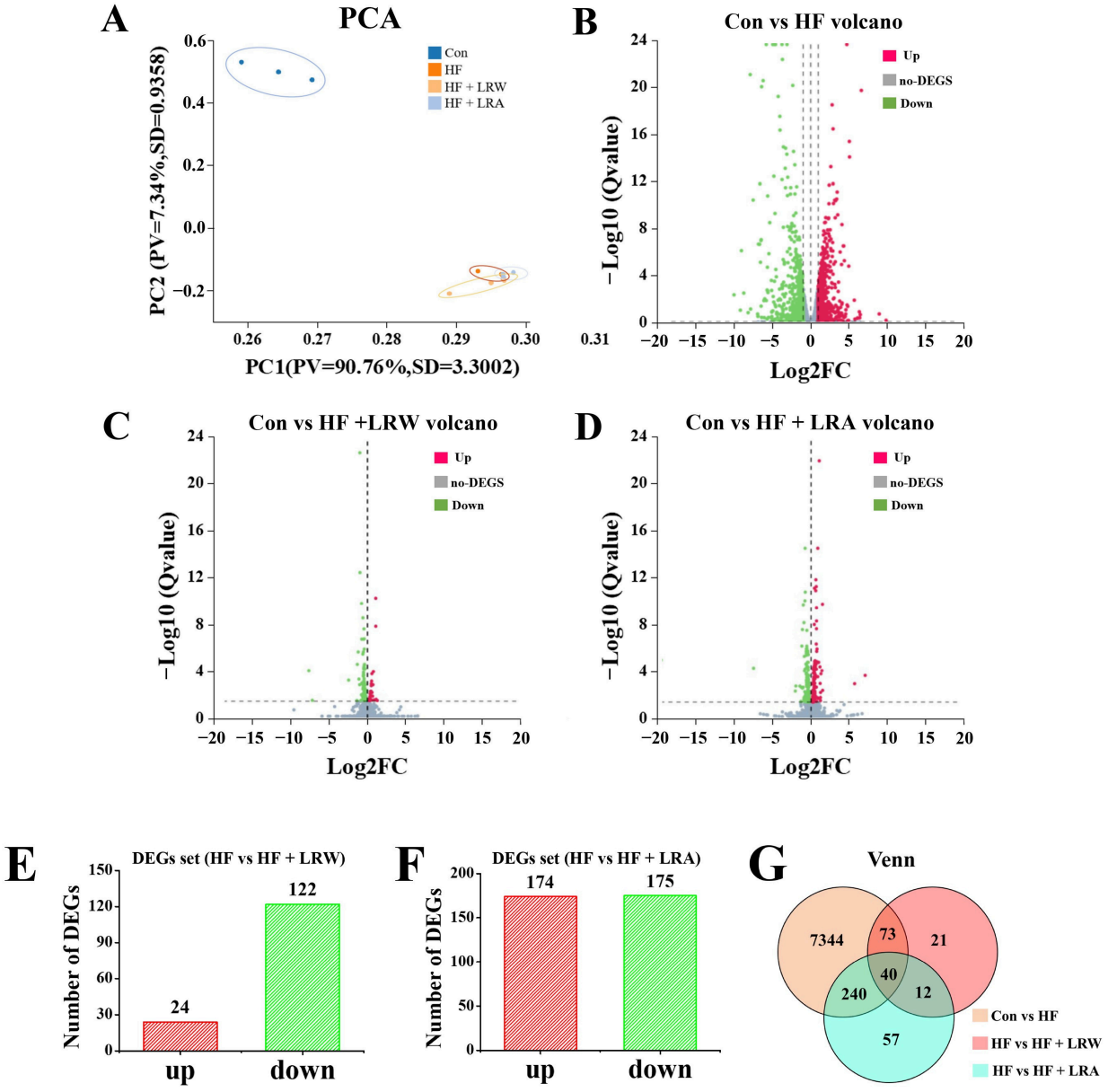

Figure 5. RNA-Seq analyses of gene expression in *Drosophila melanogaster* among the Control, HF, HF + LRW, and HF + LRA groups. (**A**) PCA of the overall transcriptional similarity and divergence among the four groups. (**B**–**D**) Volcano plots of differentially expressed genes (DEGs) for the comparisons of Con vs. HF, HF vs. HF + LRW, and HF vs. HF + LRA, respectively. (**E**,**F**) Statistical summary of upregulated and downregulated DEGs corresponding to HF vs. HF + LRW and HF vs. HF + LRA. (**G**) Venn diagram of expressed transcripts across the four experimental groups. DEGs were identified using the NOISeq method (fold change ≥ 2, adjusted Q-value < 0.05 after multiple-testing correction).

To further explore the biological functions of these DEGs, KEGG pathway enrichment analysis was performed on the significantly altered genes in LRW and LRA intervention groups (Figure 6A,B). KEGG classification results showed that the DEGs of HF vs. HF + LRW and HF vs. HF + LRA were annotated into six major pathway categories, including cellular processes, environmental information processing, genetic information processing, diseases, metabolism, and organismal systems. Further focusing on lipid metabolism-related pathways closely associated with our phenotypic indices, 5 lipid metabolism-related DEGs were enriched in the HF + LRW group, while 18 lipid metabolism-related DEGs were screened in the HF + LRA group. The significant difference in the number of lipid metabolism-related functional genes further verified that LRA exerted stronger regulatory effects on lipid metabolic transcription than LRW, which fundamentally explained the superior lipid-lowering capacity of LRA at the physiological level.

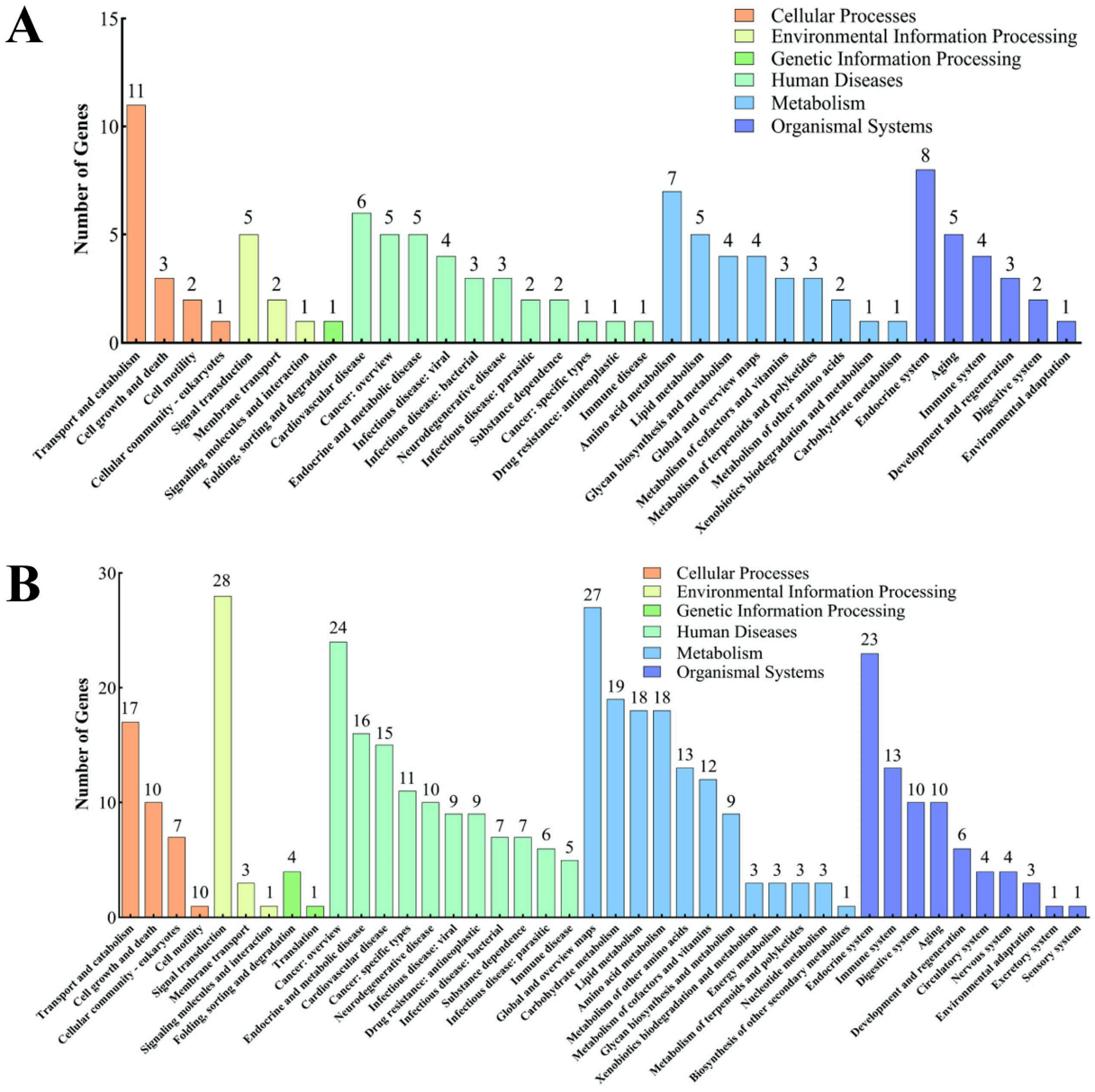

Figure 6. KEGG functional classification of differentially expressed genes (DEGs). (**A**,**B**) KEGG pathway classification of DEGs derived from the comparisons of HF vs. HF + LRW and HF vs. HF + LRA, respectively. DEGs were identified via the NOISeq algorithm. KEGG classification and enrichment analysis were performed using hypergeometric distribution combined with Benjamini–Hochberg multiple-testing correction. Pathways with Q-value < 0.05 were defined as significantly enriched.

3.6.2. Kegg Pathway Enrichment Analysis

To clarify the core molecular pathways potentially linked to the lipid-lowering effects of LRW and LRA, KEGG pathway enrichment analysis was performed on DEGs obtained from HF vs. HF + LRW and HF vs. HF + LRA comparisons. The top significantly enriched pathways ($p < 0.05$) were screened and visualized to characterize differential regulatory associations of the two polysaccharides (Figure 7). The results revealed distinct pathway enrichment patterns between LRW and LRA intervention groups.

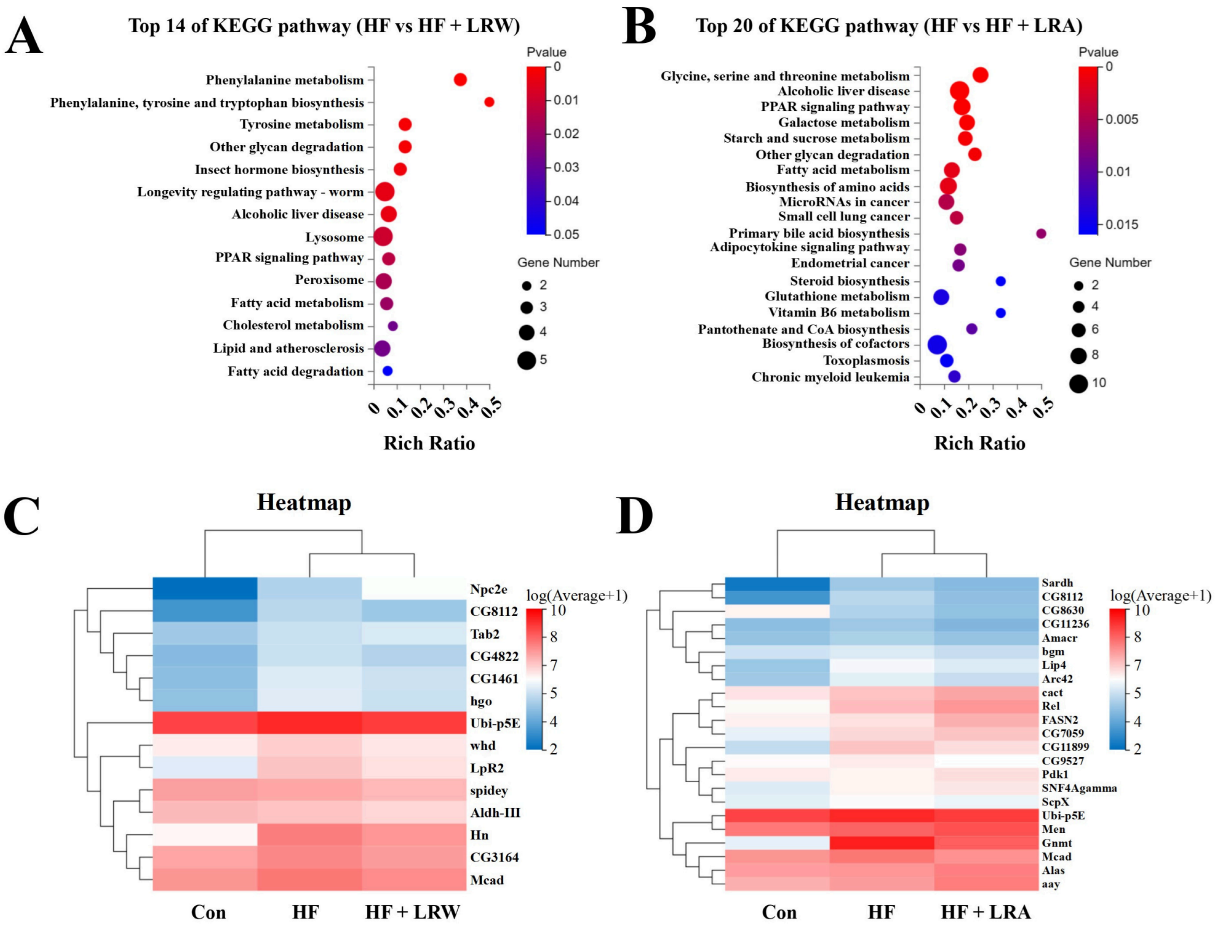

Figure 7. KEGG pathway enrichment analysis of the DEGs. (**A**) KEGG pathway enrichment of DEGs (HF vs. HF + LRW). (**B**) KEGG pathway enrichment of DEGs (HF vs. HF + LRA). Bubble size corresponds to the number of enriched DEGs, and color gradient denotes Q-value (Benjamini–Hochberg adjusted *p*-value), where redder color represents higher significance. Pathways with Q < 0.05 were defined as significantly enriched. DEGs were screened using the NOISeq method. (**C**) Heatmap showing expression changes of DEGs (HF vs. HF + LRW). (**D**) Heatmap showing expression changes of DEGs (HF vs. HF + LRA). Red: upregulated genes; blue: downregulated genes.

For the LRW intervention group, DEGs were significantly enriched in multiple lipid and amino acid metabolic pathways, including phenylalanine metabolism, phenylalanine/tyrosine/tryptophan biosynthesis, tyrosine metabolism, alcoholic liver disease, PPAR signaling pathway, fatty acid metabolism, cholesterol metabolism, lipid and atherosclerosis, and fatty acid degradation (Figure 7A). A total of 14 key DEGs involved in the above nine pathways were further analyzed via expression heatmap (Figure 7C). As summarized in Table 4, most glycolipid metabolism-related DEGs were significantly downregulated in the HF + LRW group. These transcriptional changes suggested a possible link to the altered glycolipid metabolism under high-fat stress. Notably, *Aldh-III*, a key gene responsible for metabolizing toxic aldehydes such as MDA, was differentially expressed after LRW

intervention. *Aldh-III* is closely associated with lipid peroxidation, atherosclerosis and aging-related metabolic disorders, and its expression alteration may indirectly modulate in vivo lipid homeostasis and fatty liver progression [40,41]. Therefore, the transcriptional regulation of *Aldh-III* further supports the antioxidant and lipid-regulating capacity of LRW.

Table 4. The 9 KEGG pathways and the associated 14 genes significantly affected by LRW.

Gene Name	Description	Log_2 Ratio [a]	*p* Value
Npc2e	Niemann-Pick type C-2e	1.17	6.19×10^{-12}
CG8112	CG8112	−0.47	4.22×10^{-4}
Tab2	TAK1-associated binding protein 2	0.27	4.68×10^{-4}
CG4822	CG4822	−0.39	3.94×10^{-6}
CG1461	Tyrosine aminotransferase	−0.28	3.51×10^{-4}
hgo	homogentisate 1,2-dioxygenase	−0.37	1.84×10^{-5}
Ubi-p5E	Ubiquitin-5E	−0.34	1.70×10^{-5}
whd	withered	−0.41	3.67×10^{-8}
LpR2	Lipophorin receptor 2	−0.43	1.11×10^{-9}
spidey	spidey	−0.28	3.95×10^{-4}
Aldh-III	Aldehyde dehydrogenase type III	−0.32	7.11×10^{-6}
Hn	Henna	−0.39	5.09×10^{-5}
CG3164	CG3164	−0.34	1.13×10^{-7}
Mcad	Medium-chain acyl-CoA dehydrogenase	−0.36	1.58×10^{-4}

[a] Ratio = gene expression level in the HF + LRW group: gene expression level in the HF group.

Regarding the LRA intervention group, DEGs were significantly enriched in glycine, serine and threonine metabolism, alcoholic liver disease, PPAR signaling pathway, fatty acid metabolism, primary bile acid biosynthesis, adipokine signaling pathway, and steroid biosynthesis (Figure 7B). A total of 23 key DEGs involved in these seven lipid-regulating pathways were visualized by heatmap (Figure 7D), which are summarized in Table 5. Compared with the HF group, multiple lipogenic and lipid transport-related genes, including *Sardh*, *Amacr*, *Lip4*, *ScpX*, *Ubi-p5E* and *Mcad*, were significantly downregulated in the HF + LRA group. Among them, *ScpX* participated in peroxisomal fatty acid β-oxidation and intracellular lipid transport [40,41]; its downregulation was correlated with reduced abnormal lipid accumulation and improved high-fat-induced metabolic dysfunction, which was consistent with the observed lipid-lowering phenotype. In contrast, the energy metabolism-related genes *Men* and *Pdk1* were significantly upregulated after LRA intervention. Elevated expression of Men and *Pdk1* may be associated with repressed de novo fatty acid synthesis and enhanced lipid catabolism. Collectively, these transcriptional changes were correlated with shifts in glycolipid metabolic homeostasis, which may partly underlie the alleviation of high-fat-triggered dyslipidemia [42,43].

For LRA, genes within enriched glycine–serine–threonine metabolism and PPAR signaling pathways contain multiple lipid-relevant transcripts. Among them, altered expression of lipogenic/lipid-transport genes (*Sardh*, *Lip4*, *ScpX*, *Mcad*) and energy-metabolism-related genes (*Men*, *Pdk1*) may correlate with improved lipid profiles. Specifically, Sardh knockdown has been shown to cause ectopic lipid accumulation in *Drosophila* muscle [44]; Lip4 encodes a triglyceride lipase regulated by dFOXO and NF-Y [45]; Mcad deficiency increases lipid storage [46]; and Men overexpression reduces triglyceride levels [47]. These transcript-level correlations may partly explain the superior lipid-lowering phenotype observed for LRA.

Table 5. The 7 KEGG pathways and the associated 23 genes significantly affected by LRA.

Gene Name	Description	Log_2 Ratio [b]	*p* Value
Sardh	Sarcosine dehydrogenase	−0.50	1.09×10^{-5}
CG8112	CG8112	−0.45	3.03×10^{-4}
CG8630	CG8630	−0.44	3.21×10^{-6}
CG11236	D-amino acid oxidase 2	−0.35	3.04×10^{-4}
Amacr	Alpha-methylacyl-CoA racemase	−0.38	5.59×10^{-4}
bgm	bubblegum	−0.30	7.48×10^{-5}
Lip4	Lipase 4	−0.64	2.00×10^{-7}
Arc42	Activator-recruited cofactor subunit 42	−0.32	1.21×10^{-3}
cact	cactus	0.35	3.35×10^{-7}
Rel	Relish	0.50	4.92×10^{-8}
FASN2	Fatty acid synthase 2	0.30	1.93×10^{-4}
CG7059	CG7059	0.40	2.56×10^{-5}
CG11899	CG11899	−0.25	7.38×10^{-4}
CG9527	Acyl-CoA oxidase 3	−0.40	1.09×10^{-4}
Pdk1	Phosphoinositide-dependent kinase 1	0.40	1.09×10^{-4}
SNF4Agamma	SNF4/AMP-activated protein kinase gamma subunit	0.32	1.21×10^{-3}
ScpX	Sterol carrier protein X-related thiolase	−0.31	2.91×10^{-4}
Ubi-p5E	Ubiquitin-5E	−0.30	1.93×10^{-4}
Men	Malic enzyme	0.77	1.64×10^{-15}
Gnmt	Glycine N-methyltransferase	−0.32	9.22×10^{-6}
Mcad	Medium-chain acyl-CoA dehydrogenase	−0.27	6.10×10^{-4}
Alas	Aminolevulinate synthase	0.35	1.33×10^{-4}
aay	astray	0.95	4.61×10^{-4}

[b] Ratio = gene expression level in the HF + LRA group: gene expression level in the HF group.

Our previous studies have confirmed the in vitro lipid-lowering activity of LRW and LRA. On this basis, the present study established a high-fat diet-induced hyperlipidemia *Drosophila* model to investigate the in vivo anti-hyperlipidemic, antioxidant, and lifespan-extending effects of LRW and LRA. Combined with transcriptome analysis, core differentially expressed genes and pivotal signaling pathways were screened, which revealed the distinct regulatory mechanisms of LRW and LRA in ameliorating high-fat-induced lipid metabolic disorders.

Nevertheless, several limitations of the current study should be acknowledged. First, the molecular mechanisms underlying the lipid-lowering effects of LRW and LRA were primarily inferred via transcriptomic profiling prediction without qRT-PCR or gene-level functional validation. Second, all phenotypic assays were performed on the w^{1118} *Drosophila* strain, and the transcriptomic mechanisms were exclusively identified from female flies. Accordingly, these regulatory pathways may not fully represent the molecular responses in male *Drosophila*, and it remains unclear whether the current findings are applicable to other animal models. Thus, future work will perform qRT-PCR verification for core DEGs and conduct cell or animal experiments to validate key target genes. Furthermore, follow-up studies will evaluate the practical application potential of LRW and LRA as novel natural lipid-lowering functional ingredients, to provide more solid theoretical support for their development and utilization in functional food and health care fields.

4. Conclusions

In this study, a high-fat model of *Drosophila melanogaster* was established to explore the lipid-lowering activities of lotus root polysaccharides LRW and LRA in vivo. Data

showed that both LRW and LRA significantly prolonged the lifespan of high-fat dietary *Drosophila* and effectively alleviated high-fat-triggered oxidative stress and lipid metabolic disorders, which was manifested by reduced MDA accumulation, elevated SOD and CAT activities, and decreased TC and TG levels. Comparative analysis consistently confirmed that LRA exerted more stable and superior antioxidant and lipid-lowering bioactivities than LRW, with reliable regulatory effects across different genders and developmental stages. Transcriptomic analysis further revealed their potential distinct regulatory mechanisms. LRA may improve lipid metabolism possibly by regulating lipogenic and lipid transport-related pathways via downregulation of Sardh, Amacr, Lip4, ScpX, Ubi-p5E and Mcad, and upregulation of Men and Pdk1, whereas LRW might relieve lipid peroxidation and metabolic dysfunction primarily by modulating Aldh-III. These transcriptome-based observations provide candidate targets for further functional verification. In conclusion, this study preliminarily clarified the in vivo lipid-lowering effects of LRW and LRA and potential mechanistic clues, providing a theoretical basis for the development of natural polysaccharides as functional ingredients for hyperlipidemia prevention.

Author Contributions: C.W.: Conceptualization, investigation, data analysis, writing—original draft; H.C.: Methodology, data analysis, writing—review and editing; Z.Z.: Methodology, investigation, data analysis; Y.S.: Conceptualization, methodology, supervision, writing—review and editing, funding acquisition; H.W.: Conceptualization, supervision, funding acquisition; X.X.: Conceptualization, methodology; Y.Y.: Conceptualization, methodology, supervision, funding acquisition. All authors have read and agreed to the published version of the manuscript.

Funding: This work was supported by the Science and Technology Department of Hubei Province [2025BBB041], Natural Science Foundation youth project of Hubei Province [2024AFB439] and Hubei Province Natural Science Foundation Project for Innovative Research Groups [2026AFA037].

Data Availability Statement: The original contributions presented in this study are included in the article. Further inquiries can be directed to the corresponding authors.

Conflicts of Interest: The authors declare no conflicts of interest.

References

1. Yan, Y.Y.; Wang, Q.; Sun, L.H. Extraction, Preparation, and Carboxymethyl of Polysaccharide from Lotus Root. *Food Sci. Technol.* **2022**, *42*, e17822. [CrossRef]
2. Yang, M.; Hu, D.; Cui, Z.; Li, H.; Man, C.; Jiang, Y. Lipid-Lowering Effects of Inonotus obliquus Polysaccharide In Vivo and In Vitro. *Foods* **2021**, *10*, 3085. [CrossRef] [PubMed]
3. Chen, Y.; Xu, W.; Qian, C.D.; Fenghong, H. Rapeseed Polysaccharides Alleviate Overweight Induced by High-Fat Diet with Regulation of Gut Microbiota in Rats. *Oil Crop Sci.* **2021**, *6*, 192–200. [CrossRef]
4. Wang, X.F.; Chen, X.; Tang, Y.; Wu, J.M.; Qin, D.L.; Yu, L.; Yu, C.L.; Zhou, X.G.; Wu, A.G. The Therapeutic Potential of Plant Polysaccharides in Metabolic Diseases. *Pharmaceuticals* **2022**, *15*, 1329. [CrossRef] [PubMed]
5. Chen, S.; Xi, M.; Gao, F.; Li, M.; Dong, T.; Geng, Z.; Liu, C.; Huang, F.; Wang, J.; Li, X. Evaluation of Mulberry Leaves' Hypoglycemic Properties and Hypoglycemic Mechanisms. *Front. Pharmacol.* **2023**, *14*, 1045309. [CrossRef] [PubMed]
6. Ji, X.; Yin, M.; Nie, H.; Liu, Y. A Review of Isolation, Chemical Properties, and Bioactivities of Polysaccharides from Bletilla striata. *BioMed Res. Int.* **2020**, *2020*, 5391379. [CrossRef] [PubMed]
7. Ge, H.J.; Chen, W. Cyanidin-3-O-glucoside alleviates non-alcoholic fatty liver disease through modulation of the gut microbiota. *Food Qual. Saf.* **2025**, *9*, fyaf035. [CrossRef]
8. Yin, D.F.; Zhong, Y.D.; Liu, H.; Hu, J.L. Lipid metabolism regulation by dietary polysaccharides with different structural properties. *Int. J. Biol. Macromol.* **2024**, *270*, 132253. [CrossRef] [PubMed]
9. Zheng, Z.; Gao, W.; Zhu, Z.; Li, S.; Chen, X.; Cravotto, G.; Sui, Y.; Zhou, L. Complexes of Soluble Dietary Fiber and Polyphenols from Lotus Root Regulate High-Fat Diet-Induced Hyperlipidemia in Mice. *Antioxidants* **2024**, *13*, 466. [CrossRef] [PubMed]
10. Yi, Y.; Lamikanra, O.; Sun, J.; Wang, L.M.; Min, T.; Wang, H.X. Activity Diversity Structure-Activity Relationship of Polysaccharides from Lotus Root Varieties. *Carbohydr. Polym.* **2017**, *190*, 67–76. [CrossRef] [PubMed]

11. Wang, M.; Hu, W.J.; Wang, Q.H.; Yang, B.Y.; Kuang, H.X. Extraction, purification, structural characteristics, biological activities, and application of the polysaccharides from *Nelumbo nucifera* Gaertn. (lotus): A review. *Int. J. Biol. Macromol.* **2023**, *226*, 562–579. [CrossRef] [PubMed]
12. Song, J.; Zhang, Z.; Wang, H.; Meng, Y.; Sun, Y.; Yi, Y. Study on the Structure and Lipid-Lowering Activity of Different Components of Lotus Root Polysaccharides. *Food Res. Int.* **2025**, *203*, 115801. [CrossRef] [PubMed]
13. Heidarian, Y.; Tourigny, J.P.; Fasteen, T.D.; Mahmoudzadeh, N.H.; Hurlburt, A.J.; Nemkov, T.; Reisz, J.A.; D'Alessandro, A.; Tennessen, J.M. Metabolomic Analysis of *Drosophila melanogaster* Larvae Lacking Pyruvate Kinase. *G3 Genes Genomes Genet.* **2023**, *14*, jkad228. [CrossRef] [PubMed]
14. Qian, Q.; Niwa, R. Regulation of Aging in the Fruit Fly *Drosophila melanogaster*. *Zool. Sci.* **2024**, *41*, 4–13. [CrossRef] [PubMed]
15. Hou, D.; Liu, F.; Ren, X.; Shen, Q.; Zhou, S. Protective Mechanism of Mung Bean Coat Against Hyperlipidemia in Mice Fed with a High-fat diet: Insight from Hepatic Transcriptome Analysis. *Food Funct.* **2021**, *12*, 12434–12447. [CrossRef] [PubMed]
16. Yi, Y.; Xu, W.; Fan, Y.; Wang, H.X. *Drosophila* as an Emerging Model Organism for Studies of Food-Derived Antioxidants. *Food Res.* **2021**, *143*, 110307. [CrossRef] [PubMed]
17. Vonolfen, M.C.; Altenschildesche, F.; Nam, H.J.; Brodesser, S.; Gyenis, A.; Buellesbach, J.; Lam, G.; Thummel, C.S.; Storelli, G. *Drosophila* HNF4 acts in distinct tissues to direct a switch between lipid storage and export in the gut. *Cell Rep.* **2024**, *43*, 114693. [CrossRef] [PubMed]
18. Karpova, E.K.; Bobrovskikh, M.A.; Deryuzhenko, M.A.; Shishkina, O.D.; Gruntenko, N.E. Wolbachia Effect on *Drosophila melanogaster* Lipid and Carbohydrate Metabolism. *Insects* **2023**, *14*, 14040357. [CrossRef] [PubMed]
19. Wang, H.X.; Yi, Y.; Sun, J.; Lamikanra, O.; Min, T. Fingerprint Profiling of Polysaccharides from Different Parts of Lotus Root Varieties. *RSC Adv.* **2018**, *8*, 16574–16584. [CrossRef] [PubMed]
20. Wang, L.J.; Li, Y.M.; Lei, L.; Liu, Y.W.; Wang, X.B.; Ma, K.Y.; Zhang, C.N.; Zhu, H.Y.; Zhao, Y.M.; Chen, Z.Y. Purple sweet potato anthocyanin attenuates fat-induced mortality in *Drosophila melanogaster*. *Exp. Gerontol.* **2016**, *82*, 95–103. [CrossRef] [PubMed]
21. Zhang, H.; Wang, S.; Jin, L.H. Acanthopanax senticosus Polysaccharide Regulates the Intestinal Homeostasis Disruption Induced by Toxic Chemicals in *Drosophila*. *Phytother. Res.* **2019**, *34*, 193–200. [CrossRef] [PubMed]
22. Amcheslavsky, A.; Jiang, J.; Ip, Y.T. Tissue Damage-Induced Intestinal Stem Cell Division in *Drosophila*. *Cell Stem Cell* **2009**, *4*, 49–61. [CrossRef] [PubMed]
23. Ferreira, J.; Marques, A.; Abreu, H.; Pereira, R.; Rego, A.; Pacheco, M.; Gaivão, I. Red Seaweeds Porphyra umbilicalis and Grateloupia turuturu Display Antigenotoxic and Longevity-Promoting Potential in *Drosophila melanogaster*. *Eur. J. Phycol.* **2019**, *54*, 519–530. [CrossRef]
24. Hafeez, E.; Du, D.S.; Ni, H.; Zhu, K.; Hu, F.; Zhou, J.H.; Chen, D.S. Regulation and mechanism of Bletilla striata polysaccharide on delaying aging in *Drosophila melanogaster*. *Int. J. Biol. Macromol.* **2025**, *310*, 143382. [CrossRef] [PubMed]
25. Zhou, Y.Z.; Yan, M.L.; Gao, L.; Zhang, J.Q.; Qin, X.M.; Zhang, X.; Du, G.H. Metabonomics Approach to Assessing the Metabolism Variation and Gender Gap of *Drosophila melanogaster* in Aging Process. *Exp. Gerontol.* **2017**, *98*, 110–119. [CrossRef] [PubMed]
26. Lee, H.Y.; Min, K.J. Betulinic Acid Increases the Lifespan of *Drosophila melanogaster* via Sir2 and FoxO Activation. *Nutrients* **2024**, *16*, 441. [CrossRef] [PubMed]
27. Su, J.; Jiang, L.; Wu, J.; Liu, Z.; Wu, Y. Effect of Polysaccharides Extracted from *Sipunculus nudus* (SNP) on the Lifespan and Immune Damage Repair of *Drosophila melanogaster* Exposed to Cd (VI). *Nat. Prod. Res.* **2017**, *32*, 1329–1332. [CrossRef] [PubMed]
28. Lee, S.H.; Lee, H.Y.; Yu, M.; Yeom, E.; Lee, J.H.; Yoon, A.; Lee, K.S.; Min, K.J. Extension of *Drosophila* lifespan by Korean red ginseng through a mechanism dependent on dSir2 and insulin/IGF-1 signaling. *Aging* **2019**, *11*, 9369–9387. [CrossRef] [PubMed]
29. Peng, C.; Zuo, Y.; Kwan, K.M.; Liang, Y.; Ma, K.Y.; Chan, H.Y.E.; Huang, Y.; Yu, H.; Chen, Z.-Y. Blueberry Extract Prolongs Lifespan of *Drosophila melanogaster*. *Exp. Gerontol.* **2011**, *47*, 170–178. [CrossRef] [PubMed]
30. Yang, S.; Xiu, M.; Li, X.; Shi, Y.; Wang, S.; Wan, S.; Han, S.; Yang, D.; Liu, Y.; He, J. The Antioxidant Effects of Hedysarum polybotrys Polysaccharide in Extending Lifespan and Ameliorating Aging-Related Diseases in *Drosophila melanogaster*. *Int. J. Biol. Macromol.* **2023**, *241*, 124609. [CrossRef] [PubMed]
31. Cai, C.; Cai, J.; Man, J.; Yang, Y.; Wang, Z.; Wei, C. Allomorph Distribution and Granule Structure of Lotus Rhizome C-Type Starch during Gelatinization. *Food Chem.* **2013**, *151*, 385–392. [CrossRef] [PubMed]
32. Yuan, S.; Dong, P.-Y.; Ma, H.H.; Liang, S.L.; Li, L.; Zhang, X.F. Antioxidant and Biological Activities of the Lotus Root Polysaccharide-Iron (III) Complex. *Molecules* **2022**, *27*, 7106. [CrossRef] [PubMed]
33. Luo, Y.; Xu, Y.L.; Gu, Y.P.; Gao, J.K.; Liu, X.J.; Luo, Y.H. Hypoglycemic activity and mechanism of the small bowl of Auricularia auricula-judae polysaccharides before and after degradation: A study based on a type 2 diabetes mellitus (T2DM) mouse model. *Food Qual. Saf.* **2025**, *9*, fyaf053. [CrossRef]
34. Chen, N.; Jiang, T.Y.; Xu, J.X.; Xi, W.J.; Shang, E.; Xiao, P.; Duan, J.A. The relationship between polysaccharide structure and its antioxidant activity needs to be systematically elucidated. *Int. J. Biol. Macromol.* **2024**, *270*, 132391. [CrossRef] [PubMed]
35. Fernandes, P.A.R.; Coimbra, M.A. The antioxidant activity of polysaccharides: A structure-function relationship overview. *Carbohydr. Polym.* **2023**, *314*, 120965. [CrossRef] [PubMed]

36. Han, M.; Zhang, Y.; Fang, J.; Sun, M.; Liu, Q.; Ma, Z.; Hu, D.; Gong, X.; Liu, Y.; Jin, L. Associations between Dietary Magnesium Intake and Hypertension, Diabetes, and Hyperlipidemia. *Hypertens. Res.* **2023**, *47*, 331–341. [CrossRef] [PubMed]
37. Kayode, O.T.; Rotimi, D.; Okoh, E.; Iyobhebhe, M.; Kayode, A.A.A.; Ojo, O.A. Novel Ketogenic Diet Formulation Improves Sucrose-Induced Insulin Resistance in Canton Strain *Drosophila melanogaster*. *J. Food Biochem.* **2021**, *45*, e13907. [CrossRef] [PubMed]
38. Liu, C.M.; Sun, Y.D.; Tong, X.J.; Xu, Z.C.; Xia, Q.; Xu, K. Structural characterization and hypolipidemic activity of a natural polysaccharide from *Suaeda salsa* L. *Int. J. Biol. Macromol.* **2024**, *279*, 135480. [CrossRef] [PubMed]
39. Wu, Y.; Zhang, Y.Y.; Gong, C.M.; Fan, B.C.; Li, S.Y.; Zhang, J.Y.; Li, Y.Z.; Song, X.M.; Zhang, D.D. Mechanisms and structure-activity relationship of hypolipidemic effects of polysaccharides from natural resources: A review. *Arch. Pharm. Res.* **2026**, *49*, 293–320. [CrossRef] [PubMed]
40. Li, H.M.; Sun, L.; Mittapalli, O.; Muir, W.M.; Xie, J.; Wu, J.; Schemerhorn, B.J.; Jannasch, A.; Chen, J.Y.; Zhang, F. Bowman-Birk Inhibitor Affects Pathways Associated with Energy Metabolism in *Drosophila melanogaster*. *Insect Mol. Biol.* **2010**, *19*, 303–313. [CrossRef] [PubMed]
41. Liu, Q.; Li, H.; Chen, X.; Luo, X. Dual Roles and Therapeutic Potential of ALDH3 Family Members in Cancer. *Chem.-Biol. Interact.* **2025**, *418*, 111622. [CrossRef] [PubMed]
42. Fangninou, F.F.; Yu, Z.; Li, W.; Xue, L.; Yin, D. Metastatic Effects of Perfluorooctanoic Acid (PFOA) on *Drosophila melanogaster* with Metabolic Reprogramming and Dysrhythmia in a Multigenerational Exposure Scenario. *Sci. Total Environ.* **2023**, *912*, 169305. [CrossRef] [PubMed]
43. Formica, M.; Storaci, A.M.; Bertolini, I.; Carminati, F.; Knævelsrud, H.; Vaira, V.; Vaccari, T. V-ATPase Controls Tumor Growth and Autophagy in a *Drosophila* Model of Gliomagenesis. *Autophagy* **2021**, *17*, 4442–4452. [CrossRef] [PubMed]
44. Livelo, C.; Guo, Y.M.; Daya, F.A.; Rajasekaran, V.; Varshney, S.; Le, H.D.; Barnes, S.; Panda, S.; Melkani, G.C. Time-restricted feeding promotes muscle function through purine cycle and AMPK signaling in *Drosophila* obesity models. *Nat. Commun.* **2023**, *14*, 949. [CrossRef] [PubMed]
45. Yoshioka, Y.; Anzai, K.; Kowada, R.; Hiratsuka, K.; Hirayabu, T.; Yasuda, M.; Ohkawa, Y.; Sato, T.; Suyama, M.; Yoshida, H.; et al. *Drosophila* transcription factor NF-Y suppresses transcription of the lipase 4 gene, a key gene for lipid storage. *Exp. Cell Res.* **2022**, *420*, 113307. [CrossRef] [PubMed]
46. Geronazzo, J.; Heimerl, A.; Lindell, L.; McCrimmon, S.; Stormer, C.; Horvai, B.; Johnson, I.P.; Peterson, T.M.; Zuckerman, J.; Scott, A.; et al. Characterizing fatty acid oxidation genes in *Drosophila*. *G3 Genes Genomes Genet.* **2025**, *15*, jkaf139. [CrossRef] [PubMed]
47. Kim, G.H.; Lee, Y.E.; Lee, G.H.; Cho, Y.H.; Lee, Y.N.; Jang, Y.; Paik, D.; Park, J.J. Overexpression of malic enzyme in the larval stage extends *Drosophila* lifespan. *Biochem. Biophys. Res. Commun.* **2015**, *456*, 676–682. [CrossRef] [PubMed]

Disclaimer/Publisher's Note: The statements, opinions and data contained in all publications are solely those of the individual author(s) and contributor(s) and not of MDPI and/or the editor(s). MDPI and/or the editor(s) disclaim responsibility for any injury to people or property resulting from any ideas, methods, instructions or products referred to in the content.